

ChronoSteer: Bridging Large Language Model and Time Series Foundation Model via Synthetic Data

Chengsen Wang^{1*}, Qi Qi^{1†}, Zhongwen Rao^{2†}, Lujia Pan², Jingyu Wang¹, Jianxin Liao¹

¹Beijing University of Posts and Telecommunications ²Huawei Noah's Ark Lab

{cswang, qiqi8266, wangjingyu, liaojx}@bupt.edu.cn

{raozhongwen, panlujia}@huawei.com

Abstract

Conventional forecasting methods rely on unimodal time series data, limiting their ability to exploit rich textual information. Recently, large language models (LLMs) and time series foundation models (TSFMs) have demonstrated powerful capability in textual reasoning and temporal modeling, respectively. Integrating the strengths of both to construct a multimodal model that concurrently leverages both temporal and textual information for future inference has emerged as a critical research challenge. To address the scarcity of event-series paired data, we propose a decoupled framework: an LLM is employed to transform textual events into revision instructions, which are then used to steer the output of TSFM. To implement this framework, we introduce ChronoSteer, a multimodal TSFM that can be steered through textual revision instructions, effectively bridging LLM and TSFM. Moreover, to mitigate the shortage of cross-modal instruction-series paired data, we devise a two-stage training strategy based on synthetic data. In addition, we also construct a high-quality multimodal time series forecasting benchmark to address the information leakage concerns during evaluation. After integrating with an LLM, ChronoSteer, which is trained exclusively on synthetic data, achieves a 25.7% improvement in prediction accuracy compared to the unimodal backbone and a 22.5% gain over the previous state-of-the-art multimodal method.

1 Introduction

Time series forecasting holds considerable practical value across various domains such as finance [2, 17], transportation [7, 16], and energy [31, 33]. Human experts usually combine multimodal information to make predictions. For instance, economists commonly infer market trends by analyzing both historical series and textual reports. Recently, neural network-based methods [26, 28, 46, 48] have advanced forecasting tasks owing to powerful modeling capability. However, the marked training barrier has prompted researchers to construct out-of-the-box time series foundation models (TSFMs). Although these TSFMs [1, 8, 42] exhibit robust zero-shot prediction accuracy, most are pre-trained exclusively on unimodal time series, lacking the capacity to exploit textual information.

At the same time, large language models (LLMs) exhibit remarkable zero-shot reasoning capability across various tasks [34–36], prompting growing interest in integrating them into time series analysis. Some methods [20, 49] transfer LLM weights into time series frameworks, integrating temporal and textual information by fine-tuning specific layers. However, they require individual adjustments on each dataset, lacking zero-shot generalization. Alternatively, other studies [14, 25] transform time series into string formats, leveraging prompts to enable LLMs for zero-shot forecasting in unimodal and multimodal scenarios. Nonetheless, the inherent absence of temporal capability in LLMs [11, 27]

*Work performed during the internship at Huawei.

†Corresponding authors.

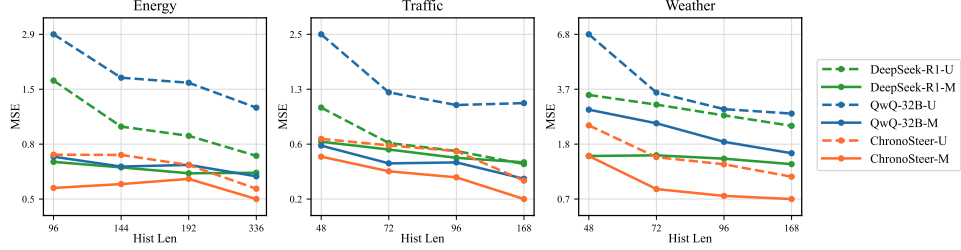


Figure 1: The prediction errors of ChronoSteer and baselines for unimodal and multimodal time series forecasting. A lower value denotes superior accuracy.

limits their effectiveness in capturing long-term dependency. While instruction fine-tuning brings partial improvements [15, 39], the constrained training data undermines broader generalization.

Figure 1 compares the zero-shot prediction accuracy of recent LLMs and TSFMs (where ChronoSteer-U denotes Chronos [1]). The results demonstrate that both temporal and textual information can improve prediction accuracy. When the historical series is short, LLMs outperform unimodal TSFMs, which lack sufficient temporal context, by leveraging their textual reasoning capability. However, as the historical series lengthens, LLMs are outperformed by unimodal TSFMs due to their limited temporal capacity for capturing long-term dependency. By integrating the textual reasoning strengths of LLMs with the temporal modeling proficiency of unimodal TSFMs, a multimodal TSFM can be developed, concurrently leveraging both temporal and textual information for future inference. Compared to fine-tuning LLMs to enhance their temporal ability, equipping lightweight unimodal TSFMs with textual comprehension offers a more computationally efficient alternative.

Textual descriptions such as background and event often present semantic complexity and data sparsity, posing significant challenges for cross-modal alignment without high-quality paired data. To address this issue, we propose a decoupled multimodal forecasting framework: leveraging an LLM with domain knowledge to transform textual events into revision instructions, which subsequently steer the output of TSFMs. By introducing textual instructions as an intermediary, the difficulty of cross-modal alignment is substantially reduced. For instance, although an event like "*Christmas Holidays*" may appear infrequently in raw paired dataset, once reinterpreted by LLMs as an instruction such as "*Elevate Peaks*", it can be more efficiently learned by TSFMs to adjust prediction output. Notably, while some time series editing models [21] have explored attribute-based series tuning, they are restricted to simple attributes and tend to neglect incorporating historical information.

Motivated by the aforementioned considerations, we introduce ChronoSteer, a multimodal TSFM that can be steered through textual revision instructions. This model preserves the unimodal TSFM backbone while integrating a lightweight branch to process textual instruction. By freezing the backbone, we reduce training overhead while maintaining the unimodal prediction performance. To address the scarcity of instruction-series paired data, we propose a two-stage training strategy based on synthetic data. Furthermore, the development of benchmarks [24, 41] for multimodal time series forecasting (MTSF) remains nascent. A notable concern is that existing datasets may overlap with those used to train LLMs, introducing risks of data leakage during evaluation. To address this issue, we adhere to the established paradigm [39] to construct MTSFBench-300, a high-quality benchmark for MTSF. This benchmark encompasses three key domains (Energy, Traffic, and Weather) and incorporates data updated to January 2025.

The contributions of our paper are summarised as follows:

- We introduce ChronoSteer, a multimodal TSFM that can be steered through textual revision instructions, effectively bridging LLM and TSFM. After integrating with an LLM, this framework concurrently leverages both temporal and textual information for future inference.
- We propose a two-stage training strategy based on synthetic data, effectively mitigating the scarcity in cross-modal alignment. Furthermore, we also construct a high-quality MTSF benchmark, advancing the development of benchmarks within this field.
- We perform extensive experiments on benchmark datasets across multiple domains, comparing ChronoSteer with mainstream baselines. The results indicate that ChronoSteer, trained exclusively on synthetic data, outperforms existing methods in various real-world scenarios.

2 Related Work

2.1 Unimodal Time Series Forecasting

As a critical real-world challenge, time series forecasting has attracted considerable attention. Early research mainly relies on statistical methods like ARIMA [3], which uses moving averages for prediction. However, these approaches often struggle with the complexity of real-world scenarios. With deep learning progress, neural network-based approaches have grown in popularity. RNNs [10, 18] capture temporal dependency through sequential architecture, yet encounter limitations such as vanishing/exploding gradients and information loss when handling long series. To overcome these challenges, researchers have introduced CNNs [40, 44] and Transformers [43, 47] to capture long-term temporal dependency. While these methods have achieved notable improvements, their training typically demands significant computational resources, domain expertise, and abundant data, posing high barriers to practical deployment. In response, TSFMs have emerged as a promising alternative. Pretrained on extensive datasets, these models [9, 13] exhibit robust generalization to support zero-shot forecasting. Nonetheless, most existing TSFMs are trained solely on unimodal time series, lacking the capacity to process multimodal inputs such as textual information, which constrains the applicability across diverse scenarios.

2.2 Multimodal Time Series Forecasting

The LLMs have brought new opportunities to time series analysis. Some methods [29, 45] transfer LLM weights to time series frameworks, integrating temporal and textual data by fine-tuning specific layers. However, they need individual adjustments for each dataset, lacking zero-shot generalization. Other studies [14, 25] convert time series into string formats, using prompts to enable LLMs for zero-shot forecasting in unimodal and multimodal scenarios. Nonetheless, the lack of temporal modeling in LLMs limits their ability to capture long-term dependency [4, 23]. While instruction fine-tuning offers partial improvements [15, 39], limited tuning data restricts broader generalization.

The time series editing task in TEdit [21] shares similarities with our work. However, TEdit focuses on adjusting series based on specified attributes, while our goal is to generate future series conditioned on both instructions and historical data. Ignoring historical information limits their control over modification extent. Moreover, TEdit supports only relatively restricted attributes, allowing only complete changes in trends or cycles. It also lacks zero-shot generalization across various datasets.

Several studies [6, 24] have introduced benchmark datasets for MTSF. However, the sources of these datasets are largely outdated. Considering the ongoing expansion of corpus size required for LLMs, existing benchmarks may have already been included in their training data. This overlap leads to information leakage during evaluation, undermining the reliability of experiment results.

3 Methodology

To enhance the distinction, a standardized notation for future series is introduced: ground truth is \mathbf{y} , unimodal prediction is $\tilde{\mathbf{y}}$, multimodal prediction is $\hat{\mathbf{y}}$, and function-transformed series is $\tilde{\mathbf{y}}$.

3.1 Problem Definition

This paper explores MTSF, aiming to concurrently leverage both temporal and textual information for future inference. Specifically, each input instance is represented by a multimodal pair (\mathbf{x}, \mathbf{e}) , where $\mathbf{x} \in \mathbb{R}^{H \times 1}$ denotes a univariate series of historical observations of length H , and \mathbf{e} indicates the corresponding textual information. The main goal is to build a generalizable multimodal zero-shot forecasting framework $\mathcal{M}(\cdot, \cdot)$ to predict future observations $\hat{\mathbf{y}} \in \mathbb{R}^{P \times 1}$ over P time steps:

$$\hat{\mathbf{y}} = \mathcal{M}(\mathbf{x}, \mathbf{e}) \quad (1)$$

When the textual information \mathbf{e} offers meaningful cues, the multimodal prediction $\mathcal{M}(\mathbf{x}, \mathbf{e})$ is expected to outperform the unimodal baseline $\mathcal{M}(\mathbf{x}, \emptyset)$:

$$\mathcal{D}(\mathcal{M}(\mathbf{x}, \mathbf{e}), \mathbf{y}) - \mathcal{D}(\mathcal{M}(\mathbf{x}, \emptyset), \mathbf{y}) < 0 \quad (2)$$

where $\mathbf{y} \in \mathbb{R}^{P \times 1}$ denotes the real future series, and $\mathcal{D}(\cdot, \cdot)$ represents a discrepancy metric. Lower values of this metric indicate better alignment between the predicted and real series.

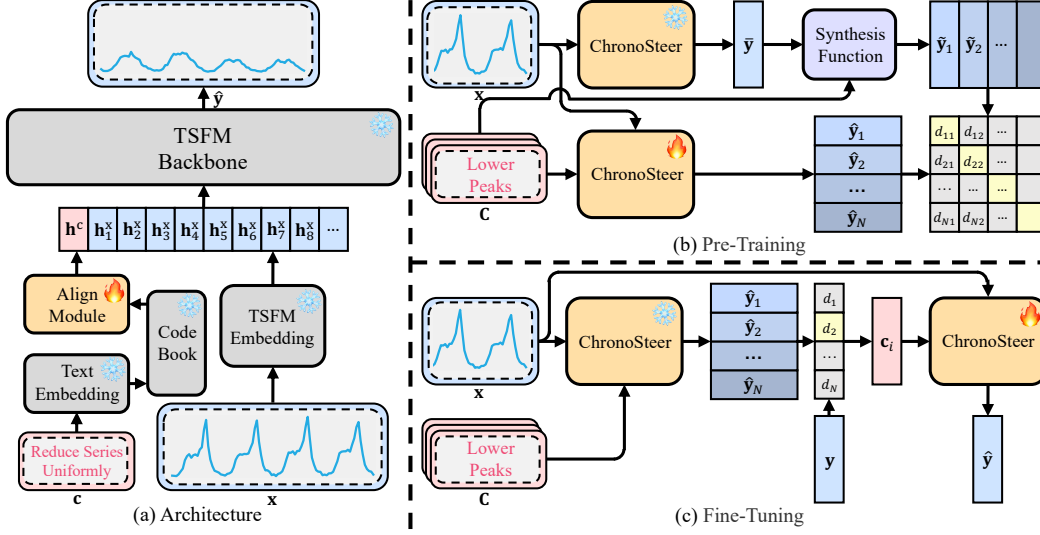


Figure 2: The overview of ChronoSteer. (a) illustrates the overall architecture, preserving the unimodal TSFM backbone while integrating a lightweight branch to process textual instruction. To mitigate the scarcity of cross-modal paired data, we introduce a two-stage training strategy: (b) synthetic data-driven pre-training followed by (c) pseudo-label-guided fine-tuning.

3.2 Framework Overview

To address the scarcity of cross-modal event-series paired data, we propose a decoupled multi-modal forecasting framework that bridges LLMs and TSFMs through textual revision instructions. Specifically, the TSFM $\mathcal{M}_{\text{series}}$ first generates unimodal predictions $\bar{y} \in \mathbb{R}^{P \times 1}$ based on historical observations \mathbf{x} . Next, an LLM $\mathcal{M}_{\text{text}}$ generates textual revision instructions \mathbf{c} by comprehensively analyzing the historical observations \mathbf{x} , the unimodal predictions \bar{y} , and the associated textual context \mathbf{e} . Finally, $\mathcal{M}_{\text{series}}$ steered by instructions \mathbf{c} produces the multimodal predictions \hat{y} . By decomposing Equation 1 into three sequential stages, the framework significantly reduces the complexity of cross-modal alignment. This technical paradigm can be formalized as:

$$\begin{aligned} \bar{y} &= \mathcal{M}_{\text{series}}(\mathbf{x}, \emptyset) \\ \mathbf{c} &= \mathcal{M}_{\text{text}}(\mathbf{x}, \bar{y}, \mathbf{e}) \\ \hat{y} &= \mathcal{M}_{\text{series}}(\mathbf{x}, \mathbf{c}) \end{aligned} \quad (3)$$

This study aims to bridge LLMs and TSFMs by developing a multimodal TSFM steered via textual revision instructions. Details on generating revision instructions, outlined in Appendix B.5, are not the primary focus. With continuous advancements in LLMs [34], semantic transformation accuracy is expected to improve steadily, offering strong support for our system.

As shown in Figure 2(a), we develop ChronoSteer, a multimodal TSFM capable of being steered by textual revision instructions. Technically, we integrate a lightweight branch to process textual instructions while preserving the unimodal TSFM backbone. Without textual instructions, ChronoSteer seamlessly reverts to the unimodal forecasting mode of backbone, ensuring robustness in practical applications. Furthermore, to address the scarcity of cross-modal instruction-series paired data, we propose a two-stage training strategy (Figures 2(b) and 2(c)) based on synthetic data. Empirical results show that ChronoSteer, trained exclusively on synthetic data, outperforms existing methods in various real-world scenarios, highlighting its substantial advantage in data efficiency.

3.3 ChronoSteer Architecture

The architecture of ChronoSteer is illustrated in Figure 2(a). Given an input pair (\mathbf{x}, \mathbf{c}) , the model first performs feature embedding. Specifically, the time series \mathbf{x} is transformed into a sequence of tokens $\mathbf{H}^x = \{\mathbf{h}_1^x, \dots, \mathbf{h}_L^x\} \in \mathbb{R}^{L \times D_{\text{series}}}$ through the embedding layer in the pre-trained unimodal

TSFM. Here, L represents the number of embedding tokens, which typically corresponds to the number of patches, and D_{series} denotes the dimension of the time series embedding. Meanwhile, the textual instruction \mathbf{c} is mapped into a text embedding $\mathbf{h}^c \in \mathbb{R}^{1 \times D_{\text{text}}}$ using a pre-trained text embedding model, where D_{text} indicates the dimension of the text embedding.

To address the complexity of textual instructions and the scarcity of paired data, we propose an anchor matching mechanism. We pre-construct a codebook $\mathbf{C} = \{\mathbf{c}_1, \dots, \mathbf{c}_N\} \in \mathbb{R}^{N \times D_{\text{text}}}$, consisting of N anchor revision instructions (detailed in Section 3.4.1, with $N = 9$ in our experiments). The cosine similarity retrieval is employed to map \mathbf{h}^c to its nearest anchor $\bar{\mathbf{h}}^c \in \mathbb{R}^{1 \times D_{\text{text}}}$:

$$\bar{\mathbf{h}}^c = \mathbf{c}_i, \text{ where } i = \arg \max_{j \in [1, N]} \cos(\mathbf{h}^c, \mathbf{c}_j) \quad (4)$$

A Multilayer Perceptron (MLP) is used for alignment of dimension and semantics:

$$\hat{\mathbf{h}}^c = \text{ReLU}(\bar{\mathbf{h}}^c \mathbf{W}_1 + \mathbf{b}_1) \mathbf{W}_2 + \mathbf{b}_2 \quad (5)$$

where $\mathbf{W}_1 \in \mathbb{R}^{D_{\text{text}} \times D_{\text{hidden}}}$ and $\mathbf{W}_2 \in \mathbb{R}^{D_{\text{hidden}} \times D_{\text{series}}}$ are weights, D_{hidden} is the hidden layer dimension. $\mathbf{b}_1 \in \mathbb{R}^{1 \times D_{\text{hidden}}}$, $\mathbf{b}_2 \in \mathbb{R}^{1 \times D_{\text{series}}}$ are biases. Notably, only this module needs to be optimized.

Given that Transformers tend to allocate more attention to the initial token [19], $\hat{\mathbf{h}}^c \in \mathbb{R}^{1 \times D_{\text{series}}}$ is concatenated to the start of \mathbf{H}^x , resulting in a combined representation $\mathbf{H} = [\hat{\mathbf{h}}^c; \mathbf{H}^x] \in \mathbb{R}^{(L+1) \times D_{\text{series}}}$. After processing by frozen TSFM backbone, the final prediction $\hat{\mathbf{y}}$ is produced.

3.4 Synthetic Data Driven Pre-training

3.4.1 Multimodal Triplet Construction

We utilize Monash Repository [12] as our training data source. A sliding window (length 160, stride 32) slices the original series into about 15M slices. Each slice is independently normalized and split into historical series \mathbf{x} (length 128) and prediction series \mathbf{y} (length 32). K-means clustering [30] is applied to optimize efficiency, like ChatTime [39], grouping samples into 1K and 100K clusters, respectively. We randomly sample one slice from each cluster to balance diversity and efficiency.

Next, predictions for the 1K slices are generated by an TSFM. The predicted and real future series are fed into an LLM to obtain open-text revision instructions. However, low quality in these instructions is observed, mainly due to the limited temporal capability of LLMs. Moreover, semantic ambiguity and computational costs further hinder the creation of large-scale aligned samples.

To address this, we refine the open-text instructions for 1K samples with expert knowledge, identifying nine core anchors. For each anchor, we design corresponding transformation functions, which are detailed in Appendix A.1.1. These functions are then applied to 100K slices, generating the ChronoSteer-100K-PT dataset, which contains 900K precisely aligned triplets $(\mathbf{x}, \mathbf{c}, \tilde{\mathbf{y}})$. The construction process is illustrated in the first row of Figure 2(b). Specifically, for each historical series \mathbf{x} , a unimodal TSFM first predicts the initial output $\bar{\mathbf{y}}$. Subsequently, the nine transformation functions, each corresponding to an anchor revision instruction within the instruction codebook $\mathbf{C} = \{\mathbf{c}_1, \dots, \mathbf{c}_N\}$, are applied to $\bar{\mathbf{y}}$, producing enhanced series $\tilde{\mathbf{Y}} = \{\tilde{\mathbf{y}}_1, \dots, \tilde{\mathbf{y}}_N\} \in \mathbb{R}^{N \times P}$.

3.4.2 Cross-Modal Contrastive Pretraining

As illustrated in the second row of Figure 2(b), for each triplets $(\mathbf{x}, \mathbf{C}, \tilde{\mathbf{Y}})$ in ChronoSteer-100K-PT, multimodal predictions $\hat{\mathbf{Y}} = \{\hat{\mathbf{y}}_1, \dots, \hat{\mathbf{y}}_N\} \in \mathbb{R}^{N \times P}$ are generated by ChronoSteer, where:

$$\hat{\mathbf{y}}_i = \text{ChronoSteer}(\mathbf{x}, \mathbf{c}_i) \quad (6)$$

In addition to the Mean Squared Error (MSE) loss \mathcal{L}_{MSE} , a contrastive loss [32] is introduced to further enhance cross-modal alignment. This loss minimizes the distance between the function output $\tilde{\mathbf{y}}_i$ and the predicted output $\hat{\mathbf{y}}_i$ for the same text instruction \mathbf{c}_i , while maximizing the distance to outputs from other instructions.

$$\mathcal{L}_{\text{Con}} = -\frac{1}{2N} \sum_{i=1}^N \left[\log \frac{\exp(\cos(\hat{\mathbf{y}}_i, \tilde{\mathbf{y}}_i))}{\sum_{j=1}^N \exp(\cos(\hat{\mathbf{y}}_i, \tilde{\mathbf{y}}_j))} + \log \frac{\exp(\cos(\tilde{\mathbf{y}}_i, \hat{\mathbf{y}}_i))}{\sum_{j=1}^N \exp(\cos(\tilde{\mathbf{y}}_i, \hat{\mathbf{y}}_j))} \right] \quad (7)$$

Finally, the composite loss function for a single instance is:

$$\mathcal{L}_{\text{total}} = \mathcal{L}_{\text{MSE}} + \alpha \mathcal{L}_{\text{Con}} \quad (8)$$

where α balances the relative contributions of these two terms.

3.5 Pseudo Label Guided Fine-Tuning

3.5.1 Pseudo Label Generation

Relying exclusively on synthetic future series $\tilde{\mathbf{y}}$ as targets limits the ceiling of the model to transformation functions. To overcome this, we incorporate the real future series \mathbf{y} as a supervised target during fine-tuning. Technically, we propose an optimal matching-based pseudo-label generation strategy, shown in the left part of Figure 2(c), to create revision instructions from unimodal predictions $\hat{\mathbf{y}}$ to align with \mathbf{y} . For each \mathbf{x} , a multimodal prediction set $\hat{\mathbf{Y}} = \{\hat{\mathbf{y}}_1, \dots, \hat{\mathbf{y}}_N\} \in \mathbb{R}^{N \times P}$ with N candidate is generated by pre-trained ChronoSteer. The prediction closest to \mathbf{y} is selected based on MSE, and its corresponding anchor revision instruction \mathbf{c}_i is assigned as the pseudo-label $\hat{\mathbf{c}}$:

$$\hat{\mathbf{c}} = \mathbf{c}_i, \text{ where } i = \arg \min_{j \in [1, N]} \text{MSE}(\hat{\mathbf{y}}_j, \mathbf{y}) \quad (9)$$

Ultimately, we construct ChronoSteer-100K-FT dataset with 100K precisely aligned triplets $(\mathbf{x}, \hat{\mathbf{c}}, \mathbf{y})$.

3.5.2 Self-Supervised Continuous Fine-Tuning

The fine-tuning process is illustrated in the right side of Figure 2(c). For each sample in ChronoSteer-100K-FT, ChronoSteer generates corresponding multimodal predictions:

$$\hat{\mathbf{y}} = \text{ChronoSteer}(\mathbf{x}, \hat{\mathbf{c}}) \quad (10)$$

During fine-tuning, parameter optimization exclusively uses MSE as the loss function.

4 Experiment

4.1 Experimental Setup

4.1.1 Dataset

The synthetic dataset from Section 3 is used to pre-train and fine-tune ChronoSteer, with data split into training and validation sets in an 8:2 ratio to reduce overfitting and aid hyperparameter optimization.

Considering the ongoing expansion of corpus size required for LLMs [34], existing benchmarks [6, 24, 39, 41] may have already been included in their training data. This overlap leads to information leakage during evaluation, undermining the reliability of experiment results. To address this, we adhere to the established paradigm [39] to construct MTSFBench-300, a high-quality benchmark for MTSF. This benchmark encompasses three key domains (Energy, Traffic, and Weather) and incorporates data updated to January 2025. Details on its construction are provided in Appendix A.1.2. We conduct evaluation experiments on MTSFBench-300, adhering to established prediction protocols [39]. Specifically, the prediction length is fixed at 1 day, while historical lengths vary across $\{2, 3, 4, 7\}$ days.

4.1.2 Baseline

To evaluate the effectiveness of ChronoSteer, we select three recent mainstream LLMs (DeepSeek-R1 [34], o3-mini [37], QwQ-32B [38]) as baselines. Additionally, to highlight our advantages in MTSF tasks, we include ChatTime-7B [39], the first dual-modal TSFM supporting time series generation and comprehension, in the comparison framework. Due to constraints on computing resources, evaluations of the LLMs are conducted via their official APIs, while ChatTime-7B and ChronoSteer are tested on our identical hardware. Further details about baselines are provided in Appendix A.2.

In our experiment, the unimodal TSFM backbone of ChronoSteer adopts Chronos-Bolt-base [1], while the text embedding model uses BGE-M3 [5]. Textual events are transformed into revision instructions via the reasoning-enhanced LLM QwQ-32B [38]. Further implementation details are provided in Appendix A.3.

Table 1: The prediction errors of ChronoSteer and baselines for unimodal and multimodal time series forecasting. A lower value denotes superior accuracy. The optimal and suboptimal results in unimodal and multimodal settings are highlighted in bold red and underlined blue, respectively.

Method		DeepSeek-R1				o3-mini				QwQ-32B				ChatTime-7B				ChronoSteer			
		Unimodal		Multimodal		Unimodal		Multimodal		Unimodal		Multimodal		Unimodal		Multimodal		Unimodal		Multimodal	
		MSE	MAE	MSE	MAE	MSE	MAE	MSE	MAE	MSE	MAE	MSE	MAE	MSE	MAE	MSE	MAE	MSE	MAE	MSE	MAE
Energy	96	1.658	0.412	<u>0.717</u>	0.276	2.874	0.574	0.751	<u>0.270</u>	3.863	0.650	0.747	0.273	<u>1.252</u>	<u>0.365</u>	0.821	0.295	0.765	0.277	0.576	0.262
	144	<u>1.005</u>	<u>0.333</u>	<u>0.682</u>	0.268	1.713	0.549	0.688	<u>0.266</u>	2.413	0.615	0.682	0.268	1.252	0.364	0.821	0.295	0.763	0.268	0.594	0.266
	192	<u>0.916</u>	<u>0.299</u>	0.649	<u>0.254</u>	1.616	0.513	0.698	0.266	1.389	0.424	<u>0.648</u>	0.264	1.252	0.364	0.821	0.295	0.697	0.259	0.619	0.253
	336	<u>0.757</u>	<u>0.280</u>	0.652	0.260	1.226	0.412	0.633	<u>0.250</u>	1.337	0.415	<u>0.630</u>	0.265	1.251	0.364	0.821	0.295	0.573	0.246	0.529	0.243
Traffic	48	1.021	<u>0.620</u>	0.642	0.536	2.461	0.891	0.606	<u>0.513</u>	1.630	0.928	0.643	0.565	<u>0.930</u>	0.681	<u>0.601</u>	0.551	0.669	0.571	0.513	0.510
	72	<u>0.630</u>	<u>0.565</u>	0.572	0.524	1.238	0.786	<u>0.462</u>	<u>0.478</u>	1.446	0.901	0.544	0.521	0.808	0.592	0.581	0.534	0.608	0.551	0.405	0.447
	96	<u>0.560</u>	<u>0.524</u>	0.504	0.502	1.055	0.729	0.469	0.481	1.372	0.883	<u>0.432</u>	<u>0.456</u>	0.666	0.581	0.452	0.463	0.559	0.522	0.365	0.429
	168	<u>0.457</u>	<u>0.463</u>	0.470	0.461	1.082	0.737	0.356	0.407	1.037	0.801	0.385	0.416	0.557	0.525	<u>0.302</u>	<u>0.350</u>	0.344	0.390	0.240	0.334
Weather	48	3.416	1.376	<u>1.537</u>	<u>0.920</u>	6.800	1.475	2.856	1.244	<u>2.392</u>	<u>1.224</u>	1.857	1.075	2.725	1.262	2.756	1.324	2.340	1.126	1.537	0.919
	72	3.038	1.332	<u>1.552</u>	<u>0.927</u>	3.516	1.342	2.404	1.117	<u>2.063</u>	<u>1.129</u>	1.766	1.011	2.698	1.292	2.577	1.281	1.511	0.967	0.902	0.724
	96	2.659	1.272	<u>1.478</u>	<u>0.891</u>	2.875	1.273	1.880	1.051	<u>1.988</u>	<u>1.041</u>	1.735	1.037	2.090	1.067	2.117	1.085	1.358	0.909	0.794	0.678
	168	2.326	1.100	<u>1.361</u>	<u>0.828</u>	2.720	1.239	1.600	0.997	1.872	1.066	1.632	1.006	<u>1.635</u>	<u>0.932</u>	1.463	0.899	1.116	0.822	0.747	0.653

Table 2: The prediction errors of ChronoSteer and editing variants for multimodal time series forecasting. A lower value denotes superior accuracy. The optimal results are highlighted in bold.

Method		ChronoSteer				Editing							
		Unimodal		Multimodal		DeepSeek-R1		o3-mini		QwQ-32B		Function	
		MSE	MAE	MSE	MAE	MSE	MAE	MSE	MAE	MSE	MAE	MSE	MAE
Energy	96	0.7650	0.2773	0.5758	0.2624	0.6273	0.2674	0.5953	0.2678	0.6024	0.2684	0.8265	0.3639
	144	0.7630	0.2681	0.5937	0.2657	0.6553	0.2721	0.6278	0.2660	0.6397	0.2721	0.8185	0.3611
	192	0.6969	0.2591	0.6194	0.2529	0.6356	0.2700	0.6203	0.2676	0.6324	0.2623	0.8018	0.3620
	336	0.5725	0.2455	0.5294	0.2427	0.5743	0.2586	0.5412	0.2499	0.5596	0.2556	0.6650	0.3877
Traffic	48	0.6685	0.5712	0.5133	0.5100	0.5471	0.5204	0.5439	0.5260	0.5393	0.5215	0.6503	0.6001
	72	0.6085	0.5508	0.4055	0.4472	0.4842	0.4832	0.4407	0.4597	0.4579	0.4683	0.4879	0.5270
	96	0.5589	0.5224	0.3653	0.4295	0.4118	0.4306	0.3982	0.4318	0.4122	0.4319	0.4974	0.5458
	168	0.3443	0.3902	0.2401	0.3336	0.3436	0.3917	0.2896	0.3862	0.3647	0.4068	0.4629	0.5346
Weather	48	2.3398	1.1258	1.5369	0.9189	1.5631	0.9349	2.0745	1.1376	1.7021	1.0316	2.1412	1.0632
	72	1.5111	0.9666	0.9016	0.7238	1.4913	0.9082	1.6166	1.0216	1.6463	0.9982	1.1460	0.8240
	96	1.3577	0.9090	0.7942	0.6780	1.3250	0.8808	1.4978	0.9194	1.4650	0.9230	1.0507	0.7839
	168	1.1158	0.8221	0.7470	0.6535	0.9301	0.7462	1.1601	0.8310	1.1708	0.8394	0.8766	0.7003

4.2 Main Result

The results in Table 1 show that ChronoSteer, trained exclusively on synthetic data, surpasses existing methods across various scenarios. When integrated with an LLM, ChronoSteer achieves a 25.7% improvement over its unimodal TSFM backbone, Chronos [1] (ChronoSteer-Unimodal), and demonstrates a 22.5% gain over the current state-of-the-art multimodal baseline, DeepSeek-R1.

As shown in Table 1, both temporal and textual information enhance prediction accuracy. Without textual data, the unimodal TSFM Chronos achieves the best performance. Even when other baselines include context, Chronos remains competitive due to its superior temporal modeling. Further analysis reveals that, for short historical series, multimodal LLMs can partially compensate for limited temporal modeling by leveraging their textual reasoning, outperforming unimodal TSFMs. However, as the length of historical series grows, temporal information becomes sufficient, and multimodal LLMs, limited in capturing long-term dependency, fall behind. This insight motivates our research: By combining the textual reasoning strengths of LLMs with the temporal modeling capability of TSFMs, we aim to develop a multimodal TSFM that concurrently leverages both temporal and textual information for future inference.

To further validate the superiority of ChronoSteer, we conduct four additional comparative experiments, as shown in Table 2. In these experiments, three LLMs modify the initial predictions \bar{y} of the unimodal TSFM by incorporating historical series and textual information. Meanwhile, the Function directly adjusts \bar{y} using the transformation function corresponding to the anchor most aligned with the textual instruction. Results show that, while the three LLMs benefit from the initial predictions and outperform their direct multimodal result in Table 1, they still fall short of ChronoSteer. Additionally, Function exhibits the weakest performance among all baselines. This comparison underscores that ChronoSteer, trained with two-stage strategy, surpasses the ceiling of transformation functions.

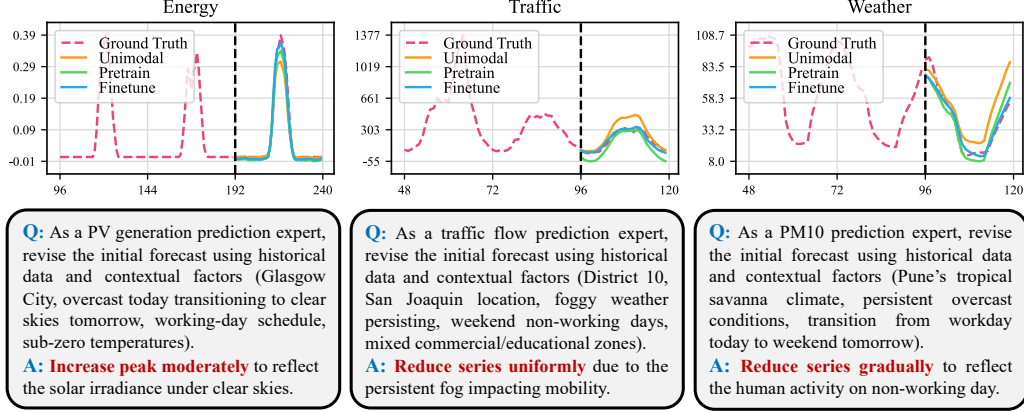


Figure 3: The illustration of prediction showcases for ChronoSteer across various training stages, including core text context and revision instructions.

Furthermore, we compare the inference speed and memory consumption of ChronoSteer with Chronos to assess its practical applicability. Detailed results in Appendix B.2 demonstrate that ChronoSteer achieves significant accuracy improvements with minimal additional computational cost. To evaluate robustness, we analyze the statistical properties of evaluation metrics across three independent runs, as shown in Appendix B.1. These results confirm the consistency and stability of ChronoSteer.

4.3 Prediction Showcase

To visually illustrate the performance of ChronoSteer across different stages, the top row of Figure 3 displays prediction results using a 1-day prediction window and a 4-day historical window (with only the last 2 days shown due to space constraints). The bottom row presents core textual information and revision instructions generated by the LLM. Further details, including the visual analysis of the anchor revision instructions, are provided in Appendix B.5. As shown in Figure 3, ChronoSteer, after two-stage fine-tuning, effectively utilizes textual revision instructions to steer the outputs of the unimodal TSFM. Furthermore, when the instructions are somewhat imprecise, ChronoSteer robustly balances them with historical series for improved performance.

In the Energy dataset, foggy weather causes a gradual decline in peaks within the historical series. Without textual context, a unimodal TSFM continues this trend, forecasting even lower peaks. However, when integrating a weather forecast indicating *"transitioning to clear skies tomorrow"*, the LLM provides revision instructions to raise the peak, steering ChronoSteer to adjust its prediction accordingly. Compared to being trained solely through pre-training, ChronoSteer fine-tuned with real future series demonstrates adjustment magnitudes that more accurately reflect real-world scenarios.

In the Traffic dataset, persistent heavy fog causes a further reduction in traffic flow peaks. Without textual information, a unimodal TSFM predicts a typical non-working day pattern similar to the previous day. When LLM provides the revision instruction *"reduce series uniformly"*, ChronoSteer adjusts its prediction accordingly. However, this instruction is imprecise, as it should target only peaks rather than the entire series. Pre-trained exclusively on synthetic series, ChronoSteer strictly follows the instructions, resulting in unrealistically troughs. In contrast, the version fine-tuned on real future series integrates the instruction with historical series, producing a more reasonable prediction.

In the Weather dataset, the transition from weekdays to non-working days reduces air pollution due to decreased human activity. Without textual information, a unimodal TSFM struggles to completely capture this pattern, leading to overestimated predictions. By integrating revision instructions, ChronoSteer improves its prediction accuracy. Compared to the pre-trained model, ChronoSteer, fine-tuned on real future series, predicts troughs and peaks more accurately.

4.4 Ablation Study

To validate the effectiveness of each component, we evaluate ChronoSteer and its variants in Table 3, where *"rp"* represents a replacement operation and *"rm"* denotes a removal operation. The

Table 3: The prediction errors of ChronoSteer and ablation variants for multimodal time series forecasting. A lower value denotes superior accuracy. The optimal results are highlighted in bold.

Method		ChronoSteer				Variant							
		Unimodal		Multimodal		rm Context		rm Contrastive		rm Finetune		rp Linear	
		MSE	MAE	MSE	MAE	MSE	MAE	MSE	MAE	MSE	MAE	MSE	MAE
Energy	96	0.7650	0.2773	0.5758	0.2624	0.5952	0.2672	0.6594	0.2992	0.6676	0.2997	0.6655	0.3246
	144	0.7630	0.2681	0.5937	0.2657	0.6264	0.2742	0.6352	0.2785	0.6816	0.2909	0.6292	0.2971
	192	0.6969	0.2591	0.6194	0.2529	0.6204	0.2717	0.6259	0.2705	0.6393	0.2788	0.6257	0.2916
	336	0.5725	0.2455	0.5294	0.2427	0.5558	0.2589	0.5557	0.2606	0.5602	0.2615	0.5339	0.2593
Traffic	48	0.6685	0.5712	0.5133	0.5100	0.5266	0.5152	0.5596	0.5303	0.5597	0.5539	0.6104	0.5846
	72	0.6085	0.5508	0.4055	0.4472	0.4156	0.4516	0.4170	0.4528	0.4093	0.4867	0.4167	0.4581
	96	0.5589	0.5224	0.3653	0.4295	0.3697	0.4329	0.3852	0.4624	0.3836	0.4657	0.3782	0.4544
	168	0.3443	0.3902	0.2401	0.3336	0.2451	0.3387	0.2558	0.3431	0.2769	0.3775	0.2455	0.3456
Weather	48	2.3398	1.1258	1.5369	0.9189	1.7852	1.0124	1.5864	0.9229	1.9594	1.0552	1.6987	0.9665
	72	1.5111	0.9666	0.9016	0.7238	1.6428	1.0090	0.9522	0.7418	1.0334	0.7809	0.9944	0.7432
	96	1.3577	0.9090	0.7942	0.6780	1.5561	0.9353	0.8580	0.7031	0.9793	0.7544	0.8824	0.7040
	168	1.1158	0.8221	0.7470	0.6535	1.0843	0.7907	0.7908	0.6768	0.8546	0.6937	0.7547	0.6556

results show that replacing or removing any component reduces prediction accuracy, confirming the architectural soundness and effectiveness of ChronoSteer. Additionally, ablation analyses on the choice of LLM, text embedding model, and the TSFM backbone are provided in Appendix B.4, offering further insights into each module.

In rm Context, context information is removed from the input to the LLM, which instead relies solely on historical series and unimodal initial predictions to generate revision instructions. Results show that the system remains robust on the stable Energy and Traffic datasets but experiences a significant decline on the unstable Weather dataset, underscoring the critical role of context.

In rm Contrastive, the contrastive learning loss is omitted during pretraining. The absence of this loss hinders the ability of ChronoSteer to effectively distinguish between different anchor revision instructions, thereby reducing cross-modal alignment performance. Specifically, removing the contrastive learning loss leads to a prediction accuracy drop of 7.3%, 5.0%, and 4.0% on the Energy, Traffic, and Weather datasets, respectively.

In rm finetune, the fine-tuning stage is omitted. Given that the model has achieved convergence after the pre-training stage, its weights are directly evaluated. By incorporating real future series as supervised targets, the fine-tuning stage breaks through the limitations of transformation functions and unlocks greater performance potential. Without the fine-tuning stage, prediction accuracy on the Energy, Traffic, and Weather datasets drops by 10.1%, 8.3%, and 16.6%, respectively.

In rp Linear, we replace the MLP in the alignment module with a linear layer, similar to LLaVA [22]. The results reveal a significant drop after this substitution. Unlike LLaVA, which uses multiple image tokens, our model represents the textual instruction as a single token. This design demands a more powerful nonlinear mapper to achieve effective cross-modal alignment. The choice of embedding the instruction into a single token stems from the lack of high-quality cross-modal alignment datasets. Using multiple tokens often leads to collapsing solutions, while a text embedding model pre-trained well is better suited for distinguishing instructions.

5 Conclusion

In this study, we focus on integrating the strengths of TSFMs and LLMs to develop a multimodal forecasting framework that concurrently leverages both temporal and textual information for future inference. We propose a decoupled framework where LLMs transform textual events into revision instructions, steering TSFM outputs and alleviating cross-modal alignment challenges. We introduce ChronoSteer, a multimodal TSFM that can be steered through textual revision instructions, effectively bridging LLM and TSFM. To address the scarcity of instruction-series paired data, we propose a two-stage training strategy based on synthetic data. We also present MTSFBench-300, a high-quality benchmark for MTSF, to minimize information leakage during evaluation. Experimental results demonstrate that ChronoSteer, trained exclusively on synthetic data, outperforms existing methods in various real-world scenarios. We believe ChronoSteer will serve as a foundation tool for MTSF, inspiring further advancements in methods and datasets within this field.

References

- [1] Abdul Fatir Ansari, Lorenzo Stella, Ali Caner Türkmen, Xiyuan Zhang, Pedro Mercado, Huibin Shen, Oleksandr Shchur, Syama Sundar Rangapuram, Sebastian Pineda-Arango, Shubham Kapoor, Jasper Zschiegner, Danielle C. Maddix, Michael W. Mahoney, Kari Torkkola, Andrew Gordon Wilson, Michael Bohlke-Schneider, and Yuyang Wang. Chronos: Learning the language of time series. *arXiv*, 2403.07815, 2024.
- [2] Adebiyi Ariyo Ariyo, Aderemi Oluyinka Adewumi, and Charles K. Ayo. Stock price prediction using the ARIMA model. In *International Conference on Computer Modelling and Simulation*, 2014.
- [3] G. E. P. Box and G. M. Jenkins. Some recent advances in forecasting and control. *Journal of the Royal Statistical Society*, 17, 1968.
- [4] Yifu Cai, Arjun Choudhry, Mononito Goswami, and Artur Dubrawski. Timeseriesexam: A time series understanding exam. *arXiv*, 2410.14752, 2024.
- [5] Jianlv Chen, Shitao Xiao, Peitian Zhang, Kun Luo, Defu Lian, and Zheng Liu. Bge m3-embedding: Multi-lingual, multi-functionality, multi-granularity text embeddings through self-knowledge distillation. *arXiv*, 2402.03216, 2024.
- [6] Wei Chen, Xixuan Hao, Yuankai Wu, and Yuxuan Liang. Terra: A multimodal spatio-temporal dataset spanning the earth. In *Neural Information Processing Systems*, 2024.
- [7] Yuzhou Chen, Ignacio Segovia-Dominguez, Baris Coskunuzer, and Yulia R. Gel. Tamps2gcnets: Coupling time-aware multipersistance knowledge representation with spatio-supra graph convolutional networks for time-series forecasting. In *International Conference on Learning Representations*, 2022.
- [8] Abhimanyu Das, Weihao Kong, Rajat Sen, and Yichen Zhou. A decoder-only foundation model for time-series forecasting. In *International Conference on Machine Learning*, 2024.
- [9] Vijay Ekambaram, Arindam Jati, Pankaj Dayama, Sumanta Mukherjee, Nam Nguyen, Wesley M. Gifford, Chandra Reddy, and Jayant Kalagnanam. Tiny time mixers (ttms): Fast pre-trained models for enhanced zero/few-shot forecasting of multivariate time series. In *Neural Information Processing Systems*, 2024.
- [10] Valentin Flunkert, David Salinas, and Jan Gasthaus. Deepar: Probabilistic forecasting with autoregressive recurrent networks. *arXiv*, 2201.00382, 2017.
- [11] Elizabeth Fons, Rachneet Kaur, Soham Palande, Zhen Zeng, Tucker Balch, Manuela Veloso, and Svitlana Vytenko. Evaluating large language models on time series feature understanding: A comprehensive taxonomy and benchmark. In *Empirical Methods in Natural Language Processing*, 2024.
- [12] Rakshitha Godahewa, Christoph Bergmeir, Geoffrey I. Webb, Rob J. Hyndman, and Pablo Montero-Manso. Monash time series forecasting archive. In *Neural Information Processing Systems*, 2021.
- [13] Mononito Goswami, Konrad Szafer, Arjun Choudhry, Yifu Cai, Shuo Li, and Artur Dubrawski. Moment: A family of open time-series foundation models. In *International Conference on Machine Learning*, 2024.
- [14] Nate Gruver, Marc Finzi, Shikai Qiu, and Andrew Gordon Wilson. Large language models are zero-shot time series forecasters. In *Neural Information Processing Systems*, 2023.
- [15] Xusen Guo, Qiming Zhang, Junyue Jiang, Mingxing Peng, Hao Yang, and Meixin Zhu. Towards responsible and reliable traffic flow prediction with large language models. *arXiv*, 2404.02937, 2024.
- [16] Hui He, Qi Zhang, Simeng Bai, Kun Yi, and Zhendong Niu. CATN: cross attentive tree-aware network for multivariate time series forecasting. In *AAAI Conference on Artificial Intelligence*, 2022.

- [17] Qi-Qiao He, Shirley Weng In Siu, and Yain-Whar Si. Instance-based deep transfer learning with attention for stock movement prediction. *Applied Intelligence*, 53, 2023.
- [18] Sepp Hochreiter and Jürgen Schmidhuber. Long short-term memory. *Neural Computation*, 9, 1997.
- [19] Ke Ji, Jiahao Xu, Tian Liang, Qiuzhi Liu, Zhiwei He, Xingyu Chen, Xiaoyuan Liu, Zhijie Wang, Junying Chen, Benyou Wang, Zhaopeng Tu, Haitao Mi, and Dong Yu. The first few tokens are all you need: An efficient and effective unsupervised prefix fine-tuning method for reasoning models. *arXiv*, 2503.02875, 2025.
- [20] Ming Jin, Shiyu Wang, Lintao Ma, Zhixuan Chu, James Y. Zhang, Xiaoming Shi, Pin-Yu Chen, Yuxuan Liang, Yuan-Fang Li, Shirui Pan, and Qingsong Wen. Timellm: Time series forecasting by reprogramming large language models. In *International Conference on Learning Representations*, 2024.
- [21] Baoyu Jing, Shuqi Gu, Tianyu Chen, Zhiyu Yang, Dongsheng Li, Jingrui He, and Kan Ren. Towards editing time series. In *Neural Information Processing Systems*, 2024.
- [22] Haotian Liu, Chunyuan Li, Qingyang Wu, and Yong Jae Lee. Visual instruction tuning. In *Neural Information Processing Systems*, 2023.
- [23] Haoxin Liu, Chenghao Liu, and B. Aditya Prakash. A picture is worth A thousand numbers: Enabling llms reason about time series via visualization. *arXiv*, 2411.06018, 2024.
- [24] Haoxin Liu, Shangqing Xu, Zhiyuan Zhao, Ling kai Kong, Harshavardhan Kamarthi, Aditya B. Sasanur, Megha Sharma, Jiaming Cui, Qingsong Wen, Chao Zhang, and B. Aditya Prakash. Time-mmd: A new multi-domain multimodal dataset for time series analysis. In *Neural Information Processing Systems*, 2024.
- [25] Haoxin Liu, Zhiyuan Zhao, Jindong Wang, Harshavardhan Kamarthi, and B. Aditya Prakash. Lstprompt: Large language models as zero-shot time series forecasters by long-short-term prompting. In *Findings of the Association for Computational Linguistics*, 2024.
- [26] Yong Liu, Tengge Hu, Haoran Zhang, Haixu Wu, Shiyu Wang, Lintao Ma, and Mingsheng Long. itransformer: Inverted transformers are effective for time series forecasting. In *International Conference on Learning Representations*, 2024.
- [27] Mike A. Merrill, Mingtian Tan, Vinayak Gupta, Thomas Hartvigsen, and Tim Althoff. Language models still struggle to zero-shot reason about time series. In *Findings of the Association for Computational Linguistics*, 2024.
- [28] Yuqi Nie, Nam H. Nguyen, Phanwadee Sinthong, and Jayant Kalagnanam. A time series is worth 64 words: Long-term forecasting with transformers. In *International Conference on Learning Representations*, 2023.
- [29] Zijie Pan, Yushan Jiang, Sahil Garg, Anderson Schneider, Yuriy Nevmyvaka, and Dongjin Song. S2IP-LLM: semantic space informed prompt learning with LLM for time series forecasting. In *International Conference on Machine Learning*, 2024.
- [30] F. Pedregosa, G. Varoquaux, A. Gramfort, V. Michel, B. Thirion, O. Grisel, M. Blondel, P. Prettenhofer, R. Weiss, V. Dubourg, J. Vanderplas, A. Passos, D. Cournapeau, M. Brucher, M. Perrot, and E. Duchesnay. Scikit-learn: Machine learning in python. *Journal of Machine Learning Research*, 12, 2011.
- [31] Tiago Pinto, Isabel Praça, Zita A. Vale, and José Silva. Ensemble learning for electricity consumption forecasting in office buildings. *Neurocomputing*, 423, 2021.
- [32] Alec Radford, Jong Wook Kim, Chris Hallacy, Aditya Ramesh, Gabriel Goh, Sandhini Agarwal, Girish Sastry, Amanda Askell, Pamela Mishkin, Jack Clark, Gretchen Krueger, and Ilya Sutskever. Learning transferable visual models from natural language supervision. In *International Conference on Machine Learning*, 2021.

- [33] Tárík S. Salem, Karan Kathuria, Heri Ramampiaro, and Helge Langseth. Forecasting intra-hour imbalances in electric power systems. In *AAAI Conference on Artificial Intelligence*, 2019.
- [34] DeepSeek-AI Team. Deepseek-r1: Incentivizing reasoning capability in llms via reinforcement learning. *arXiv*, 2501.12948, 2025.
- [35] Meta Team. Llama 2: Open foundation and fine-tuned chat models. *arXiv*, 2307.09288, 2023.
- [36] OpenAI Team. GPT-4 technical report. *arXiv*, 2303.08774, 2023.
- [37] OpenAI Team. Openai o3-mini, 2025. URL <https://openai.com/index/openai-o3-mini>.
- [38] Qwen Team. Qwq-32b: Embracing the power of reinforcement learning, 2025. URL <https://qwenlm.github.io/blog/qwq-32b/>.
- [39] Chengsen Wang, Qi Qi, Jingyu Wang, Haifeng Sun, Zirui Zhuang, Jinming Wu, Lei Zhang, and Jianxin Liao. Chattime: A unified multimodal time series foundation model bridging numerical and textual data. In *AAAI Conference on Artificial Intelligence*, 2025.
- [40] Huiqiang Wang, Jian Peng, Feihu Huang, Jince Wang, Junhui Chen, and Yifei Xiao. MICN: multi-scale local and global context modeling for long-term series forecasting. In *International Conference on Learning Representations*, 2023.
- [41] Andrew Robert Williams, Arjun Ashok, Étienne Marcotte, Valentina Zantedeschi, Jithendaraa Subramanian, Roland Riachi, James Requeima, Alexandre Lacoste, Irina Rish, Nicolas Chapados, and Alexandre Drouin. Context is key: A benchmark for forecasting with essential textual information. *arXiv*, 2410.18959, 2024.
- [42] Gerald Woo, Chenghao Liu, Akshat Kumar, Caiming Xiong, Silvio Savarese, and Doyen Sahoo. Unified training of universal time series forecasting transformers. In *International Conference on Machine Learning*, 2024.
- [43] Haixu Wu, Jiehui Xu, Jianmin Wang, and Mingsheng Long. Autoformer: Decomposition transformers with auto-correlation for long-term series forecasting. In *Neural Information Processing Systems*, 2021.
- [44] Haixu Wu, Tengge Hu, Yong Liu, Hang Zhou, Jianmin Wang, and Mingsheng Long. Timesnet: Temporal 2d-variation modeling for general time series analysis. In *International Conference on Learning Representations*, 2023.
- [45] Zhijian Xu, Yuxuan Bian, Jianyuan Zhong, Xiangyu Wen, and Qiang Xu. Beyond trend and periodicity: Guiding time series forecasting with textual cues. *arXiv*, 2405.13522, 2024.
- [46] Ailing Zeng, Muxi Chen, Lei Zhang, and Qiang Xu. Are transformers effective for time series forecasting? In *AAAI Conference on Artificial Intelligence*, 2023.
- [47] Yunhao Zhang and Junchi Yan. Crossformer: Transformer utilizing cross-dimension dependency for multivariate time series forecasting. In *International Conference on Learning Representations*, 2023.
- [48] Haoyi Zhou, Shanghang Zhang, Jieqi Peng, Shuai Zhang, Jianxin Li, Hui Xiong, and Wancai Zhang. Informer: Beyond efficient transformer for long sequence time-series forecasting. In *AAAI Conference on Artificial Intelligence*, 2021.
- [49] Tian Zhou, Peisong Niu, Xue Wang, Liang Sun, and Rong Jin. One fits all: Power general time series analysis by pretrained lm. In *Neural Information Processing Systems*, 2023.

A Detailed Experimental Setup

A.1 Dataset

A.1.1 ChronoSteer-100K

Algorithm 1 Synthetic Function

```
import numpy as np
from sklearn.preprocessing import MinMaxScaler

def normalize(series):
    scaler = MinMaxScaler()
    normed = (scaler.fit_transform(series.reshape(-1, 1)).reshape(-1) - 0.5) * 2
    return normed, scaler

def denormalize(series, scaler):
    return scaler.inverse_transform(series.reshape(-1, 1) / 2 + 0.5).reshape(-1)

def tanh_curve(length, factor, n=8):
    return np.tanh(np.linspace(0, n, length)) * factor

def keep_unchanged(series):
    return series

def increase_trend(series, min_factor=0.2, max_factor=0.8):
    series, scaler = normalize(series)
    trend = tanh_curve(len(series), np.random.uniform(min_factor, max_factor))
    return denormalize(series + trend, scaler)

def reduce_trend(series, min_factor=0.2, max_factor=0.8):
    series, scaler = normalize(series)
    trend = tanh_curve(len(series), np.random.uniform(min_factor, max_factor))
    return denormalize(series - trend, scaler)

def expand_amplitude(series, min_factor=0.2, max_factor=0.8):
    series, scaler = normalize(series)
    factor = tanh_curve(len(series), np.random.uniform(min_factor, max_factor))
    return denormalize(series * (1 + factor), scaler)

def compress_amplitude(series, min_factor=0.2, max_factor=0.8):
    series, scaler = normalize(series)
    factor = tanh_curve(len(series), np.random.uniform(min_factor, max_factor))
    return denormalize(series * (1 - factor), scaler)

def elevate_peaks(series, min_factor=0.1, max_factor=0.4):
    series, scaler = normalize(series)
    amp = np.random.uniform(min_factor, max_factor)
    return denormalize((series + 1) * (1 + amp) - 1, scaler)

def lower_peaks(series, min_factor=0.1, max_factor=0.4):
    series, scaler = normalize(series)
    amp = np.random.uniform(min_factor, max_factor)
    return denormalize((series + 1) * (1 - amp) - 1, scaler)

def raise_troughs(series, min_factor=0.1, max_factor=0.4):
    series, scaler = normalize(series)
    amp = np.random.uniform(min_factor, max_factor)
    return denormalize((series - 1) * (1 - amp) + 1, scaler)

def deepen_troughs(series, min_factor=0.1, max_factor=0.4):
    series, scaler = normalize(series)
    amp = np.random.uniform(min_factor, max_factor)
    return denormalize((series - 1) * (1 + amp) + 1, scaler)
```

After applying clustering sampling and anchor extraction to the Monash Repository³, we successfully obtained 100K high-quality time series slices and identified nine core anchor revision instructions: "Keep Unchanged", "Increase Trend", "Reduce Trend", "Expand Amplitude", "Compress Amplitude", "Elevate Peaks", "Lower Peaks", "Raise Troughs" and "Deepen Troughs". Each slice is independently

³<https://forecastingdata.org>

Table 4: The statistics of each sub-dataset. A lower ADF test statistic denotes more stationary series.

Domain	Num	Period	Freq	Hist	Pred	ADF	Information
Energy	100	2025-01-01~2025-01-31	30 minutes	{96, 144, 192, 336}	48	-8.08	photovoltaic generation
Traffic	100	2025-01-01~2025-01-31	1 hour	{48, 72, 96, 168}	24	-5.68	traffic flow
Weather	100	2025-01-01~2025-01-31	1 hour	{48, 72, 96, 168}	24	-3.77	particulate matter

normalized and split into historical series \mathbf{x} and prediction series (length 32). For each historical series \mathbf{x} , a unimodal TSFM first predicts the initial output $\bar{\mathbf{y}}$. Subsequently, the nine transformation functions (in Algorithm 1), each corresponding to an anchor revision instruction within the instruction codebook \mathbf{C} , are applied to $\bar{\mathbf{y}}$, producing enhanced series $\bar{\mathbf{Y}}$.

A.1.2 MTSFBench-300

In contrast to the abundant benchmark datasets available in domains such as text-image and text-video, the development of benchmark datasets for MTSF remains comparatively underdeveloped. Considering the ongoing expansion of corpus size required for LLMs, existing benchmarks may have already been included in their training data. This overlap leads to information leakage during evaluation, undermining the reliability of experiment results. To address this, we adhere to the established paradigm to construct MTSFBench-300, a high-quality benchmark for MTSF. This benchmark encompasses three key domains (Energy, Traffic, and Weather) and incorporates data updated to January 2025. Detailed statistical characteristics are provided in Table 4.

The Energy dataset is constructed using the UK PV generation system. The raw data consists of 317 GSPs, from which seven faulty units are excluded after a data integrity assessment. To ensure spatial representativeness, 100 GSPs are selected through clustering based on geographic coordinates. The PV generation series is recorded at a 30-minute resolution and includes contextual information such as background, city, forecast-only weather (to prevent future information leakage), and date. Time series slices are generated using a 14-day sliding window (7 days of historical data and 7 days for prediction) with a one-day stride. Finally, 100 representative samples are retained by clustering based on multidimensional characteristics, including geospatial information, weather conditions, and holidays. The dataset exhibits substantial diurnal variability, with non-zero values occurring exclusively during daylight hours. Appendix B.5.2 provides corresponding text prompts and visual representations. Raw data collection mainly depends on the following sources:

- PV generation series: <https://www.solar.sheffield.ac.uk>
- GSP information: https://api.solar.shed.ac.uk/pvlive/api/v4/gsp_list
- Latitude and longitude information: https://www.neso.energy/data-portal/gis-boundaries-gb-grid-supply-points/gsp_-_gnode_-_direct_connect_-_region_lookup_20181031
- Weather information: <https://open-meteo.com/en/docs/historical-forecast-api>
- Holiday information: <https://pypi.org/project/holidays>

The Traffic dataset is derived from the highway sensor network in California. Following LargeST, 8,600 valid nodes are selected from an initial pool of 18,954 sensors. After integrating POIs, spatial clustering is performed based on geographic coordinates and POI information, yielding 100 representative nodes. Hourly traffic flow series is collected and supplemented with contextual information, including background, city, forecast-only weather (to prevent future information leakage), and date. Time series slices are generated using a 14-day sliding window (7 days of historical data and 7 days for prediction) with a one-day stride. Subsequently, 100 representative samples are retained through multidimensional clustering, considering factors such as geospatial information, POIs, weather conditions, and holidays. The dataset exhibits a relatively stable distribution. Appendix B.5.3 provides corresponding text prompts and visual representations. Raw data collection mainly depends on the following sources:

- Traffic flow series: <https://pems.dot.ca.gov>
- Sensor information: <https://github.com/liuxu77/LargeST>
- POI information: <https://overpass-turbo.eu>

- City information: <https://pypi.org/project/geopy>
- Weather information: <https://open-meteo.com/en/docs/historical-forecast-api>
- Holiday information: <https://pypi.org/project/holidays>

The Weather dataset focuses on monitoring PM10 concentrations in major global cities. From a total of 47,868 cities, 771 core cities with populations exceeding one million are selected. With clustering sampling based on geographic coordinates, climate types, and altitude, 100 representative cities are chosen for further analysis. Hourly PM10 concentration series is collected and enriched with contextual information, including background, forecast-only weather (to prevent future information leakage), and date. Time series slices are generated using a 14-day sliding window (7 days of historical data and 7 days for prediction) with a one-day stride. Finally, 100 representative samples are selected through clustering, considering multidimensional attributes such as geospatial information, climate, elevation, weather conditions, and holidays. The dataset demonstrates significant non-stationarity. Appendix B.5.4 provides corresponding text prompts and visual representations. Raw data collection mainly depends on the following sources:

- PM10 concentration series: <https://open-meteo.com/en/docs/air-quality-api>
- City information: <https://simplemaps.com/data/world-cities>
- Climate information: https://en.wikipedia.org/wiki/K%C3%B6ppen_climate_classification
- Elevation information: <https://www.gpsvisualizer.com/geocoder/elevation.html>
- Weather information: <https://open-meteo.com/en/docs/historical-forecast-api>
- Holiday information: <https://pypi.org/project/holidays>

A.2 Baseline

To evaluate the effectiveness of ChronoSteer, we select three mainstream LLMs (DeepSeek-R1, o3-mini, QwQ-32B) as baselines. Additionally, to highlight our advantages in MTSF tasks, we include ChatTime-7B, the first dual-modal TSFM supporting time series generation and comprehension, in the comparison framework. Due to constraints on computing resources, evaluations of the LLMs are conducted via their official APIs, while ChatTime-7B and ChronoSteer are tested on our identical hardware. The characteristics of the selected baselines are as follows:

- DeepSeek-R1: The first large-scale reasoning model, with over 100 billion parameters, specializes in mathematics, programming, and logical reasoning tasks. Released in January 2025, its knowledge is current up to July 2024. We use the API provided on its official website ⁴, with all parameters set to default values.
- o3-mini: A lightweight reasoning model with image understanding and multi-tool integration capability, excelling in solving mathematical and scientific problems. Released in January 2025, its knowledge is current up to June 2024. We use the API provided on its official website ⁵, with all parameters set to default values.
- QwQ-32B: A reinforcement learning-based model performs comparable to DeepSeek-R1 with 671B parameters in mathematical and programming tasks, using only 32B parameters. Released in March 2025, its knowledge is current up to December 2024. We use the API provided on its official website ⁶, with all parameters set to default values.
- ChatTime-7B: A multimodal foundation model tailored for time series analysis, fine-tuned from LLaMA-2-7B using LoRA, supports dual-modal input and output of series and text. Released in December 2024, its knowledge is current up to July 2023. We use the weight provided on its official website ⁷, with all parameters set to default values.

⁴<https://platform.deepseek.com/usage>

⁵<https://openai.com/api>

⁶<https://bailian.console.aliyun.com>

⁷<https://huggingface.co/ChengsenWang/ChatTime-1-7B-Chat>

Table 5: The statistical metrics of prediction errors for ChronoSteer in unimodal and multimodal time series forecasting under different settings. A lower value denotes superior robustness.

LLM	Align	Hist	Energy		Traffic		Weather	
			MSE	MAE	MSE	MAE	MSE	MAE
\times	\checkmark	96 / 48	0.576 ± 0.000	0.264 ± 0.002	0.509 ± 0.006	0.505 ± 0.007	1.521 ± 0.022	0.919 ± 0.000
		144 / 72	0.592 ± 0.002	0.265 ± 0.001	0.398 ± 0.010	0.445 ± 0.003	0.900 ± 0.002	0.722 ± 0.002
		192 / 96	0.606 ± 0.019	0.253 ± 0.000	0.363 ± 0.003	0.428 ± 0.002	0.806 ± 0.016	0.685 ± 0.010
		336 / 168	0.529 ± 0.001	0.244 ± 0.001	0.243 ± 0.004	0.335 ± 0.002	0.765 ± 0.026	0.663 ± 0.013
\checkmark	\times	96 / 48	0.573 ± 0.055	0.266 ± 0.028	0.462 ± 0.072	0.474 ± 0.050	1.496 ± 0.037	0.913 ± 0.056
		144 / 72	0.602 ± 0.016	0.265 ± 0.043	0.414 ± 0.012	0.458 ± 0.015	0.916 ± 0.020	0.744 ± 0.029
		192 / 96	0.620 ± 0.004	0.253 ± 0.002	0.378 ± 0.074	0.425 ± 0.047	0.803 ± 0.020	0.680 ± 0.082
		336 / 168	0.517 ± 0.017	0.243 ± 0.000	0.235 ± 0.037	0.332 ± 0.013	0.760 ± 0.020	0.665 ± 0.096
\checkmark	\checkmark	96 / 48	0.589 ± 0.062	0.264 ± 0.014	0.461 ± 0.074	0.474 ± 0.051	1.569 ± 0.033	0.922 ± 0.061
		144 / 72	0.621 ± 0.013	0.264 ± 0.034	0.413 ± 0.011	0.460 ± 0.018	0.907 ± 0.035	0.719 ± 0.036
		192 / 96	0.613 ± 0.025	0.252 ± 0.006	0.363 ± 0.082	0.424 ± 0.051	0.794 ± 0.021	0.680 ± 0.082
		336 / 168	0.522 ± 0.049	0.243 ± 0.001	0.237 ± 0.023	0.333 ± 0.001	0.762 ± 0.018	0.660 ± 0.083

A.3 Implementation

In our experiment, the unimodal TSFM backbone of ChronoSteer is based on Chronos-Bolt-base⁸ with an embedding dimension of 768, while the text embedding model uses BGE-M3⁹, which has an embedding dimension of 1024. Textual events are transformed into revision instructions using the LLM QwQ-32B¹⁰. The prompts for generating these textual revision instructions and their corresponding answers are detailed in Appendix B.5. Additionally, ablation studies on the choice of LLM, text embedding model, and TSFM backbone are provided in Appendix B.4, offering further insights into the impact of each module.

During both the pre-training and fine-tuning stages of ChronoSteer, the Adam optimizer is consistently employed. The model is trained for up to 100 epochs, with early stopping triggered if the validation loss does not decrease over 10 consecutive epochs, mitigating overfitting. In the pre-training stage, which involves contrastive learning tasks with multiple anchor revision instructions, a batch size of 32 is used. During fine-tuning, the batch size is increased to 256. Through grid search, the optimal hyperparameters for ChronoSteer are determined: an initial learning rate of 0.001 (selected from {0.0001, 0.0005, 0.001, 0.005}), a hidden layer dimension of 1024 in the alignment module (selected from {512, 1024, 2048, 4096}), and a contrastive loss weight of 0.001 during pre-training (selected from {0.0001, 0.001, 0.01, 0.1}). Appendix B.3 provides a detailed analysis of each hyperparameter.

All experiments are conducted using Python 3.10.13 and PyTorch 2.1.2. The performance is evaluated using mean squared error (MSE) and mean absolute error (MAE), where lower values indicate better model performance. To facilitate open science and community collaboration, we will make all data, source code, and pre-trained weight checkpoints publicly accessible following the release. These resources will offer substantial support for subsequent research.

B Full Experimental Result

B.1 Robustness Analysis

Table 5 presents the statistical properties of the evaluation metrics for ChronoSteer across three independent runs to assess its robustness. Three experiment setups are designed to evaluate system performance under varying conditions:

- In the first experiment, the revision instructions derived from textual events are fixed, while ChronoSteer undergoes three independent runs.
- In the second experiment, ChronoSteer remains constant, and QwQ-32B is invoked three times independently to generate different revision instructions from the same textual events.

⁸<https://huggingface.co/autogluon/chronos-bolt-base>

⁹<https://huggingface.co/BAAI/bge-m3>

¹⁰<https://huggingface.co/Qwen/QwQ-32B>

Table 6: The inference time and memory usage of ChronoSteer for unimodal and multimodal time series forecasting. A lower value denotes superior efficiency.

Method		Unimodal				Multimodal			
		MSE	MAE	Time (s, 10^{-3})	Parameter (MB, 10^2)	MSE	MAE	Time (s, 10^{-3})	Parameter (MB, 10^2)
Energy	96	0.7650	0.2773	8.3308	7.8313	0.5758	0.2624	8.0037	7.9014
	144	0.7630	0.2681	7.9592	7.8313	0.5937	0.2657	7.9445	7.9014
	192	0.6969	0.2591	7.9486	7.8313	0.6194	0.2529	7.9377	7.9014
	336	0.5725	0.2455	8.0592	7.8313	0.5294	0.2427	7.9942	7.9014
Traffic	48	0.6685	0.5712	7.9344	7.8313	0.5133	0.5100	7.8697	7.9014
	72	0.6085	0.5508	7.9545	7.8313	0.4055	0.4472	7.9334	7.9014
	96	0.5589	0.5224	7.9584	7.8313	0.3653	0.4295	7.8958	7.9014
	168	0.3443	0.3902	7.9950	7.8313	0.2401	0.3336	7.9604	7.9014
Weather	48	2.3398	1.1258	7.9395	7.8313	1.5369	0.9189	7.8763	7.9014
	72	1.5111	0.9666	7.9526	7.8313	0.9016	0.7238	7.9336	7.9014
	96	1.3577	0.9090	7.9658	7.8313	0.7942	0.6780	7.9007	7.9014
	168	1.1158	0.8221	7.9970	7.8313	0.7470	0.6535	7.9665	7.9014

- In the third experiment, neither the revision instructions nor ChronoSteer is fixed, enabling three fully independent runs.

The results in Table 5 reveal that when the revision instructions are fixed, ChronoSteer demonstrates exceptional robustness, with a minimal standard deviation indicating high output consistency. Furthermore, due to its fine-tuning on real future series, which enables instruction correction based on historical series (as detailed in Section 4.3), the system maintains low error levels even when the revision instructions vary. This highlights its strong consistency and stability.

B.2 Efficiency Evaluation

To assess the practicality of ChronoSteer in real-world scenarios, we compare it with its unimodal backbone, Chronos, focusing on inference speed and memory consumption. The results in Table 6 demonstrate that by integrating a lightweight textual instruction processing branch and employing a training strategy that freezes the backbone network, ChronoSteer achieves a significant accuracy improvement of 25.7% with negligible additional computational cost. Remarkably, its inference speed remains nearly identical to that of Chronos, even showing a slight enhancement, while memory usage increases by only 0.9%.

B.3 Hyperparameter Analysis

To assess the sensitivity of ChronoSteer to hyperparameter selections, we evaluate its prediction performance under various configurations. The historical length is set to 4 days and the prediction length to 1 day. The key hyperparameters examined include the learning rate, the contrastive loss weight during pre-training, and the hidden layer dimension of MLP in alignment module.

The contrastive loss weight during the pre-training stage directly affects the ability of ChronoSteer to distinguish anchor revision instructions. A lower weight shifts optimization focus toward MSE loss, reducing discriminative power. Conversely, a higher weight leads to over-reliance on contrastive loss, potentially hindering the capture of fine-grained temporal characteristics. As shown in Figure 4(a), increasing the contrastive loss weight initially boosts prediction accuracy on the Energy and Traffic datasets before declining, consistent with theoretical expectations. Notably, the unstable Weather dataset shows robustness to this parameter, achieving peak performance at a weight of 0.1.

The learning rate is a key parameter affecting model training. A small learning rate may cause slow convergence and risk trapping the model in local optima, while a large learning rate, though speeding up convergence, can lead to instability or divergence. As shown in Figure 4(b), ChronoSteer consistently improves prediction accuracy on the Traffic and Weather datasets as the learning rate increases, revealing a clear pattern. However, due to the high proportion of zero-value samples in the Energy dataset, it shows greater sensitivity to the learning rate and achieves optimal performance at a learning rate of 0.001.

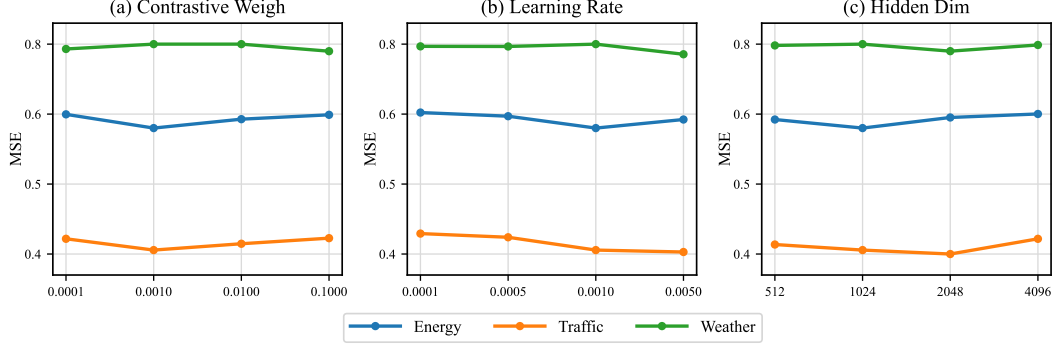


Figure 4: The prediction errors of ChronoSteer with various hyperparameter configurations for multimodal time series forecasting. A lower value denotes superior accuracy.

Table 7: The prediction errors of ChronoSteer with various large language models for multimodal time series forecasting. A lower value denotes superior prediction accuracy. The optimal results are highlighted in bold.

Method		Unimodal		Qwen2.5-32B		QwQ-32B		Qwen2.5-32B-VL		QVQ-72B	
		MSE	MAE	MSE	MAE	MSE	MAE	MSE	MAE	MSE	MAE
Energy	96	0.7650	0.2773	0.6033	0.2652	0.5758	0.2624	0.5848	0.2697	0.7262	0.2719
	144	0.7630	0.2681	0.6052	0.2672	0.5937	0.2657	0.5588	0.2606	0.7197	0.2662
	192	0.6969	0.2591	0.6026	0.2581	0.6194	0.2529	0.5421	0.2484	0.6658	0.2580
	336	0.5725	0.2455	0.5430	0.2450	0.5294	0.2427	0.5293	0.2425	0.5644	0.2431
Traffic	48	0.6685	0.5712	0.5174	0.5106	0.5133	0.5100	0.5131	0.5128	0.5566	0.5249
	72	0.6085	0.5508	0.4383	0.4564	0.4055	0.4472	0.3902	0.4350	0.4114	0.4471
	96	0.5589	0.5224	0.3740	0.4371	0.3653	0.4295	0.3621	0.4273	0.3912	0.4388
	168	0.3443	0.3902	0.2883	0.3407	0.2401	0.3336	0.3278	0.3783	0.3353	0.3852
Weather	48	2.3398	1.1258	1.8406	1.0547	1.5369	0.9189	1.9660	1.0863	1.8210	1.0714
	72	1.5111	0.9666	1.1577	0.8148	0.9016	0.7238	1.0755	0.8166	1.1612	0.8210
	96	1.3577	0.9090	1.0433	0.7952	0.7942	0.6780	0.9235	0.7412	0.9679	0.7598
	168	1.1158	0.8221	1.0011	0.7816	0.7470	0.6535	0.8661	0.7084	0.9422	0.7381

The dimension of the hidden vector influences the learning capacity and representational power. A smaller dimension reduces computational overhead but may hinder the capture of complex characteristics. Conversely, a larger hidden vector improves expressiveness and generalization. However, this often comes at the cost of higher computation and an elevated risk of overfitting, particularly when training data is limited or of poor quality. As shown in Figure 4(c), prediction accuracy across all datasets initially increases and then decreases as the hidden dimension grows, consistent with theory. Optimal performance is typically achieved when it falls between 1024 and 2048.

B.4 Ablation Study

B.4.1 Ablation Study on Large Language Model

In the primary experiment, the LLM QwQ-32B is employed to transform textual events into revision instructions. To assess how different LLMs affect the prediction accuracy of the system, this section replaces QwQ-32B with alternative models for comparison. Specifically, four models are tested: standard LLM Qwen2.5-32B¹¹, reasoning-enhanced LLM QwQ-32B¹², standard vLLM Qwen2.5-32B-VL¹³, and reasoning-enhanced vLLM QVQ-72B-Preview¹⁴.

As shown in Table 7, the reasoning-enhanced LLM QwQ-32B demonstrates significantly higher instruction transformation accuracy than the standard LLM Qwen2.5-32B, particularly on unstable

¹¹<https://huggingface.co/Qwen/Qwen2.5-32B>

¹²<https://huggingface.co/Qwen/QwQ-32B>

¹³<https://huggingface.co/Qwen/Qwen2.5-VL-32B-Instruct>

¹⁴<https://huggingface.co/Qwen/QVQ-72B-Preview>

Table 8: The prediction errors of ChronoSteer with various text embedding models for multimodal time series forecasting. A lower value denotes superior prediction accuracy. The optimal results are highlighted in bold.

Method		Unimodal		all-MiniLM-L6-v2 (384)		Voyage-3-lite (512)		BGE-M3 (1024)		NV-Embed-v2 (4096)	
		MSE	MAE	MSE	MAE	MSE	MAE	MSE	MAE	MSE	MAE
Energy	96	0.7650	0.2773	0.7437	0.2852	0.6888	0.2966	0.5758	0.2624	0.6018	0.2914
	144	0.7630	0.2681	0.6489	0.2756	0.6842	0.2976	0.5937	0.2657	0.6024	0.2865
	192	0.6969	0.2591	0.6226	0.2595	0.5771	0.2668	0.6194	0.2529	0.5814	0.2715
	336	0.5725	0.2455	0.5224	0.2457	0.5623	0.2592	0.5294	0.2427	0.5363	0.2545
Traffic	48	0.6685	0.5712	0.7621	0.6331	0.8169	0.6657	0.5133	0.5100	0.4464	0.4945
	72	0.6085	0.5508	0.5836	0.5398	0.4511	0.4780	0.4055	0.4472	0.4369	0.4708
	96	0.5589	0.5224	0.5149	0.5204	0.5181	0.5334	0.3653	0.4295	0.3897	0.4440
	168	0.3443	0.3902	0.3013	0.3855	0.2915	0.3624	0.2401	0.3336	0.2573	0.3458
Weather	48	2.3398	1.1258	2.2819	1.1343	1.4945	0.9222	1.5369	0.9189	1.4795	0.9062
	72	1.5111	0.9666	1.4402	0.8921	1.1365	0.8185	0.9016	0.7238	1.0612	0.7793
	96	1.3577	0.9090	1.3035	0.8635	0.9582	0.7485	0.7942	0.6780	0.8343	0.6818
	168	1.1158	0.8221	1.0226	0.7604	0.8738	0.7125	0.7470	0.6535	0.8540	0.6919

datasets. Improvements in prediction accuracy reach 1.4%, 3.5%, and 18.1% on the Energy, Traffic, and Weather datasets, respectively.

Previous research indicates that LLMs struggle to comprehend temporal characteristics effectively. Representing time series as images and leveraging vLLMs can better capture complex temporal patterns. Based on this, we introduce the standard vLLM Qwen2.5-32B-VL and the reasoning-enhanced vLLM QVQ-72B-Preview for comparative experiments. Results show that the standard vLLM Qwen2.5-32B-VL achieves competitive performance, closely matching the reasoning-enhanced LLM QwQ-32B. For instance, on the Energy dataset, its prediction accuracy outperforms QwQ-32B by 3.2%, while on the Traffic dataset, it trails by only 3.2%. However, the accuracy of Qwen2.5-32B-VL on the unstable Weather dataset is 17.7% lower than QwQ-32B. This may be due to cross-modal fine-tuning reducing textual reasoning capability. Despite this, it still outperforms the standard LLM Qwen2.5-32B by 3.6%. Surprisingly, the reasoning-enhanced vLLM QVQ-72B-Preview performs the worst across all datasets. This underperformance may stem from the preview version being in an optimization phase, where insufficient stability leads to suboptimal results.

B.4.2 Ablation Study on Embedding Model

In the primary experiment, the text embedding model BGE-M3 is employed to transform textual revision instructions into high-dimension embedding vectors. To examine the impact of different text embedding models on system prediction accuracy, BGE-M3 is replaced with several widely used alternatives. Specifically, four models are selected: all-MiniLM-L6-v2¹⁵, Voyage-3-lite¹⁶, BGE-M3¹⁷, and NV-Embed-v2¹⁸. Based on the MTEB Leaderboard¹⁹, these models show a progressive increase in embedding dimensions and representational capability.

As shown in Table 8, prediction accuracy improves incrementally with enhanced embedding capability. However, despite NV-Embed-v2 having nearly ten times the parameters of BGE-M3, its performance does not significantly surpass that of BGE-M3. This may be due to the high dimension of NV-Embed-v2. With its larger embedding size, the synthetic dataset may be insufficient to effectively train an alignment module of this scale, limiting the full potential of the model.

B.4.3 Ablation Study on Time series Foundation Model

In the primary experiment, the unimodal TSFM Chronos-Bolt-base serves as the backbone for ChronoSteer. To explore how varying scales of unimodal TSFM affect prediction accuracy, Chronos-Bolt-base is replaced with several other models differing in parameter size. Specifically, four models

¹⁵<https://huggingface.co/sentence-transformers/all-MiniLM-L6-v2>

¹⁶<https://www.voyageai.com>

¹⁷<https://huggingface.co/BAAI/bge-m3>

¹⁸<https://huggingface.co/nvidia/NV-Embed-v2>

¹⁹<https://huggingface.co/spaces/mteb/leaderboard>

Table 9: The prediction errors of ChronoSteer with various time series foundation models for unimodal and multimodal time series forecasting. A lower value denotes superior prediction accuracy. The optimal results are highlighted in bold.

Method		Chronos-Bolt-tiny				Chronos-Bolt-mini				Chronos-Bolt-small				Chronos-Bolt-base			
		Unimodal		Multimodal		Unimodal		Multimodal		Unimodal		Multimodal		Unimodal		Multimodal	
		MSE	MAE	MSE	MAE	MSE	MAE	MSE	MAE	MSE	MAE	MSE	MAE	MSE	MAE	MSE	MAE
Energy	96	0.653	0.265	0.631	0.259	0.659	0.259	0.639	0.251	0.803	0.274	0.715	0.271	0.765	0.277	0.576	0.262
	144	0.665	0.262	0.607	0.258	0.686	0.260	0.596	0.254	0.775	0.262	0.688	0.258	0.763	0.268	0.594	0.266
	192	0.611	0.256	0.561	0.253	0.670	0.256	0.561	0.251	0.802	0.261	0.644	0.260	0.697	0.259	0.619	0.253
	336	0.578	0.250	0.532	0.246	0.645	0.255	0.519	0.243	0.768	0.255	0.653	0.252	0.573	0.246	0.529	0.243
Traffic	48	0.632	0.559	0.469	0.482	0.662	0.577	0.553	0.568	0.685	0.584	0.571	0.519	0.669	0.571	0.513	0.510
	72	0.620	0.552	0.465	0.478	0.605	0.554	0.383	0.450	0.613	0.547	0.412	0.476	0.608	0.551	0.405	0.447
	96	0.596	0.538	0.389	0.430	0.564	0.526	0.381	0.460	0.593	0.526	0.425	0.492	0.559	0.522	0.365	0.429
	168	0.351	0.403	0.299	0.379	0.353	0.399	0.249	0.342	0.351	0.397	0.257	0.360	0.344	0.390	0.240	0.334
Weather	48	2.027	1.081	1.602	0.963	2.246	1.141	1.643	0.942	2.137	1.116	1.588	0.941	2.340	1.126	1.537	0.919
	72	1.599	0.994	1.041	0.783	1.747	1.024	1.027	0.774	1.616	0.992	1.015	0.762	1.511	0.967	0.902	0.724
	96	1.381	0.920	0.908	0.733	1.409	0.934	0.864	0.711	1.461	0.942	0.872	0.705	1.358	0.909	0.794	0.678
	168	1.142	0.821	0.794	0.674	1.124	0.826	0.798	0.675	1.169	0.838	0.756	0.649	1.116	0.822	0.747	0.653

are tested: Chronos-Bolt-tiny²⁰, Chronos-Bolt-mini²¹, Chronos-Bolt-small²², and Chronos-Bolt-base²³, with parameter counts increasing progressively.

The experiment results in Table 9 show that prediction accuracy does not clearly improve with an increase in the parameter count of the backbone, for either unimodal or multimodal tasks. However, our method demonstrates strong adaptability across backbones with different scales, consistently boosting multimodal prediction accuracy relative to unimodal results in all cases. Specifically, applying the proposed method improves prediction accuracy for Chronos-Bolt-tiny, Chronos-Bolt-mini, Chronos-Bolt-small, and Chronos-Bolt-base by 19.8%, 23.1%, 22.5%, and 25.6%, respectively.

B.5 Prediction Showcase

B.5.1 Prediction Showcase on Code Book

Figure 5 illustrates the adjustment effects of nine anchor revision instructions. As shown, pre-training objectives rely on future series synthesized via functions, so adjustments by ChronoSteer after pre-training generally align with these transformation functions. However, after fine-tuning on real future series using pseudo-labeling techniques, ChronoSteer surpasses the limitations of these functions. It balances historical data and revision instructions better, yielding more accurate and realistic predictions. This greatly enhances its practical value in real-world scenarios.

B.5.2 Prediction Showcase on Energy

Figure 6 presents the comprehensive prediction visualization for the Energy dataset, comparing a 4-day historical series with a 1-day predicted series. The predictions include results from the unimodal TSFM, ChronoSteer after pre-training, and ChronoSteer after fine-tuning. Additionally, a detailed description of the prompt, reasoning process, and revision instructions for the Energy dataset is provided to support result replication. The foggy weather causes a gradual decline in peaks within the historical series. Without textual context, a unimodal TSFM continues this trend, forecasting even lower peaks. However, when integrating a weather forecast indicating "*transitioning to clear skies tomorrow*", the LLM provides revision instructions to raise the peak, steering ChronoSteer to adjust its prediction accordingly. Compared to being trained solely through pre-training, ChronoSteer fine-tuned demonstrates adjustment magnitudes that more accurately reflect real-world scenarios.

B.5.3 Prediction Showcase on Traffic

Figure 7 presents the comprehensive prediction visualization for the Traffic dataset, comparing a 4-day historical series with a 1-day predicted series. The predictions include results from the

²⁰<https://huggingface.co/amazon/chronos-bolt-tiny>

²¹<https://huggingface.co/autogluon/chronos-bolt-mini>

²²<https://huggingface.co/autogluon/chronos-bolt-small>

²³<https://huggingface.co/autogluon/chronos-bolt-base>

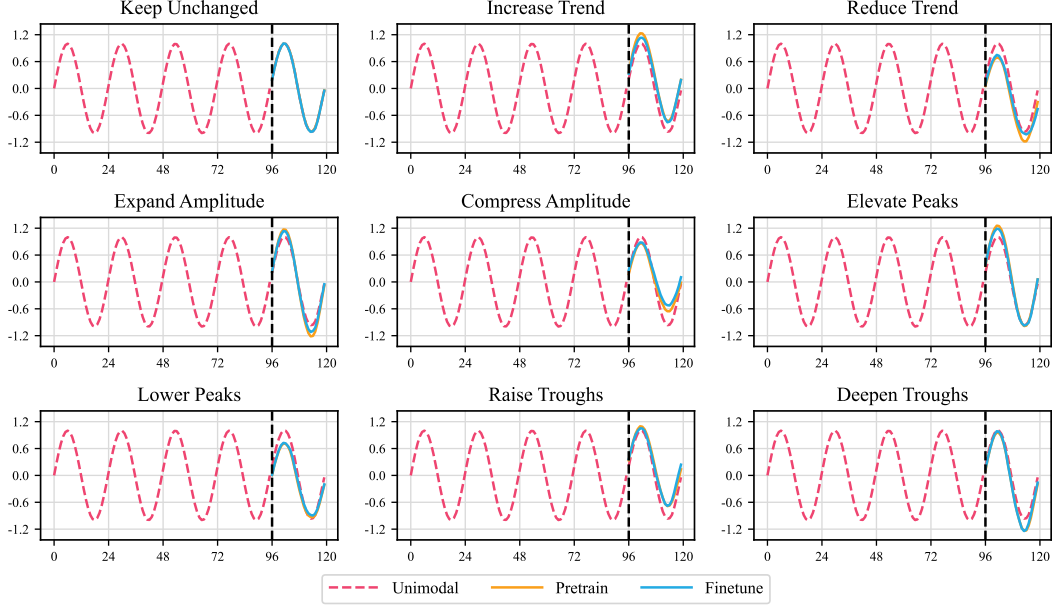
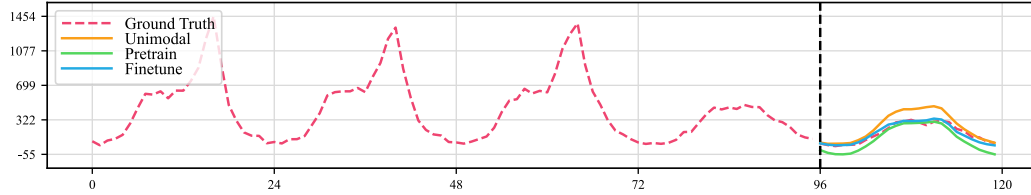


Figure 5: The illustration of prediction showcases for ChronoSteer across various training stages on the anchor revision instructions.

unimodal TSFM, ChronoSteer after pre-training, and ChronoSteer after fine-tuning. Additionally, a detailed description of the prompt, reasoning process, and revision instructions for the Traffic dataset is provided to support result replication. The persistent heavy fog causes a further reduction in traffic flow peaks. Without textual information, a unimodal TSFM predicts a typical non-working day pattern similar to the previous day. When LLM provides the revision instruction *"reduce series uniformly"*, ChronoSteer adjusts its prediction accordingly. However, this instruction is imprecise, as it should target only peaks rather than the entire series. Pre-trained exclusively on synthetic series, ChronoSteer strictly follows the instructions, resulting in unrealistically troughs. In contrast, the version fine-tuned on real future series integrates the instruction with historical series, producing a more reasonable prediction. This error-correction capability significantly enhances the practical value of ChronoSteer in real-world scenarios.

B.5.4 Prediction Showcase on Weather

Figure 8 presents the comprehensive prediction visualization for the Weather dataset, comparing a 4-day historical series with a 1-day predicted series. The predictions include results from the unimodal TSFM, ChronoSteer after pre-training, and ChronoSteer after fine-tuning. Additionally, a detailed description of the prompt, reasoning process, and revision instructions for the Weather dataset is provided to support result replication. The transition from weekdays to non-working days reduces air pollution due to decreased human activity. Without textual information, a unimodal TSFM struggles to completely capture this pattern, leading to overestimated predictions. By integrating revision instructions, ChronoSteer improves its prediction accuracy. Compared to the pre-trained model, ChronoSteer, fine-tuned on real future series, predicts troughs and peaks more accurately.



Q: You are a traffic flow prediction expert. Your task is to revise the initial predicted traffic flow in the future generated by the forecasting model. This involves considering both historical observed data and relevant contextual information to ensure the predictions align more closely with real-world conditions.

Some important information is listed as follows:

- Location: District 10, San Joaquin, California, USA, along the eastbound SR4-E freeway, lane 3.
- Region: Covers transportation areas, commercial areas and educational areas within a 5 km radius.
- Today's weather: Fog, with temperatures ranging from a low of 0 degrees Celsius to a high of 15 degrees Celsius.
- Tomorrow's weather: Fog, with temperatures ranging from a low of -1 degrees Celsius to a high of 14 degrees Celsius.
- Today's date: 2025-01-18, Saturday, a non-working day.
- Tomorrow's date: 2025-01-19, Sunday, a non-working day.

The traffic flow for the past 96 time steps (2025-01-15 00:00:00 to 2025-01-18 23:00:00, collected every hour) are as follows: [88, 44, 96, 114, 158, 283, 453, 607, 598, 634, 558, 642, 641, 748, 892, 1212, 1454, 937, 484, 314, 185, 149, 147, 66, 80, 64, 110, 111, 145, 270, 396, 589, 625, 634, 634, 671, 625, 795, 944, 1208, 1331, 881, 563, 315, 212, 163, 151, 80, 75, 62, 84, 112, 140, 236, 407, 533, 548, 662, 610, 639, 623, 821, 1097, 1260, 1377, 923, 631, 488, 316, 204, 163, 112, 75, 59, 69, 60, 71, 104, 189, 191, 290, 385, 456, 436, 458, 441, 485, 463, 461, 375, 318, 297, 245, 162, 130, 114].

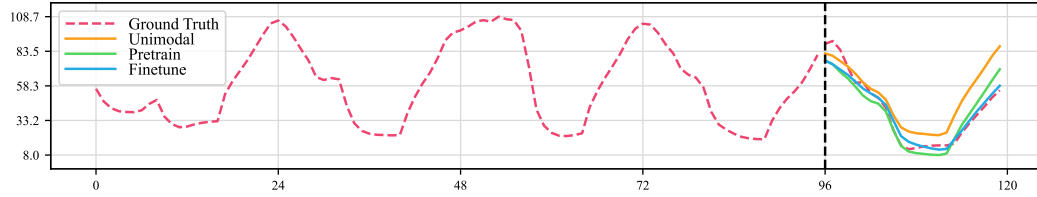
The initial predicted traffic flow for the next 24 time steps (2025-01-19 00:00:00 to 2025-01-19 23:00:00) are as follows: [74, 60, 60, 63, 68, 99, 139, 205, 289, 368, 412, 439, 439, 448, 462, 472, 448, 367, 282, 220, 169, 119, 97, 68].

Analyze the provided information carefully and determine how the initial predicted traffic flow series should be adjusted to better reflect expected real-world conditions, considering time series properties such as trend, amplitude, peak, and trough. Provide only one concise and actionable revision instruction without including explanation, number, time, or specific domain term (e.g., traffic flow, power generation). If no adjustment is necessary, maintaining the original prediction is also acceptable..

T: Okay I'm assessing San Joaquin's District 10 weekend traffic patterns under persistent fog. Historical data shows weekday peaks around 1454 dropping to ~1097 on prior weekends. Initial prediction's 472 peak for tomorrow (Sunday) seems conflicting – weekend patterns should drive lower volumes than weekdays, but fog's additional impact isn't accounted for. Freezing temps with fog suggest two compounding effects: reduced discretionary travel (lower baseline) and slower peak-hour throughput. However, commercial zones within 5km might maintain essential traffic flow. Key tension: should weekend-adjusted prediction be further reduced for weather, or does the model already incorporate weekend behavior? Noticing historical weekend troughs around 114 align with initial prediction's 74-start, but fog's visibility constraints likely suppress afternoon peaks below typical weekend levels. Decision path: moderately scale down entire prediction curve, preserving weekend waveform but compressing amplitude to reflect mobility hesitancy and icy road cautions, while maintaining essential commercial/residential movement patterns.

A: Reduce the series values uniformly due to persistent fog impacting mobility.

Figure 7: The illustration of prediction showcases for ChronoSteer across various training stages on Traffic sub-dataset, including complete context prompt, thought content, and revision instructions.



Q: You are a particulate matter PM10 prediction expert. Your task is to revise the initial predicted particulate matter PM10 in the future generated by the forecasting model. This involves considering both historical observed data and relevant contextual information to ensure the predictions align more closely with real-world conditions.

Some important information is listed as follows:

- Location: Pune, India.
- Geography: Characterized by tropical savanna climate (tropical wet and dry climate) and an average elevation of 559 meters.
- Today's weather: Overcast, with temperatures ranging from a low of 17 degrees Celsius to a high of 32 degrees Celsius.
- Tomorrow's weather: Overcast, with temperatures ranging from a low of 16 degrees Celsius to a high of 32 degrees Celsius.
- Today's date: 2025-01-24, Friday, a working day.
- Tomorrow's date: 2025-01-25, Saturday, a non-working day.

The particulate matter PM10 for the past 96 time steps (2025-01-21 00:00:00 to 2025-01-24 23:00:00, collected every hour) are as follows: [56.2, 47.1, 42.1, 39.9, 39.3, 39.2, 40.5, 45.2, 48.1, 36.0, 30.5, 28.2, 28.7, 30.4, 31.5, 32.2, 32.6, 52.4, 61.9, 69.6, 77.5, 86.6, 95.7, 103.8, 105.9, 101.5, 93.8, 85.0, 76.6, 64.7, 62.6, 64.0, 63.1, 44.1, 31.2, 25.6, 23.5, 22.7, 22.5, 22.3, 22.5, 38.3, 50.4, 60.1, 68.2, 78.7, 91.5, 97.1, 98.7, 101.5, 105.0, 106.2, 105.0, 108.7, 106.9, 106.2, 98.5, 72.2, 41.0, 29.3, 24.1, 22.0, 21.8, 22.5, 23.8, 42.8, 54.4, 64.0, 72.6, 81.5, 92.2, 99.9, 103.6, 102.9, 96.9, 88.5, 82.0, 70.8, 66.4, 64.3, 56.9, 39.5, 30.2, 26.4, 23.5, 21.2, 20.1, 19.6, 19.4, 32.8, 42.1, 49.1, 54.5, 61.2, 70.5, 80.8].

The initial predicted particulate matter PM10 for the next 24 time steps (2025-01-25 00:00:00 to 2025-01-25 23:00:00) are as follows: [81.7, 80.1, 76.3, 72.4, 67.2, 60.8, 56.2, 53.5, 48.3, 37.0, 28.3, 25.3, 24.0, 23.5, 22.9, 22.6, 24.4, 36.7, 47.4, 56.1, 63.9, 71.8, 80.4, 87.3].

Analyze the provided information carefully and determine how the initial predicted particulate matter PM10 series should be adjusted to better reflect expected real-world conditions, considering time series properties such as trend, amplitude, peak, and trough. Provide only one concise and actionable revision instruction without including explanation, number, time, or specific domain term (e.g., traffic flow, power generation). If no adjustment is necessary, maintaining the original prediction is also acceptable.

T: Okay I'm looking at Pune's PM10 data where tomorrow shifts from working Friday to non-working Saturday. Historical patterns show weekday peaks around 103.8 with overnight drops to ~19.4. The model's prediction starts tomorrow at 81.7 which sharply contradicts yesterday's closing low of 19.4. Weekend factor creates tension: reduced traffic/industry should lower particulates, but stable overcast weather might maintain accumulation. Key conflict surfaces, should the prediction maintain typical morning rebound pattern or flatten due to activity changes? Historicals show cyclical behavior where PM10 rebuilds daily regardless of calendar, but weekends likely weaken this regeneration. My adjustment logic: bridge the gap between yesterday's 19.4 and predicted 81.7 starting point by moderating the morning surge, compress the peak below 87.3 while preserving gradual daytime rise, account for decreased human emissions without eliminating baseline atmospheric particulate behavior. Essentially scale down the prediction curve vertically while keeping its temporal shape, acknowledging both weekend reductions and persistent meteorological conditions affecting pollutant dispersion.

A: Reduce the predicted PM10 values gradually throughout the day, especially dampening the morning rise and evening peak to reflect reduced human activity on a non-working day.



Figure 8: The illustration of prediction showcases for ChronoSteer across various training stages on Weather sub-dataset, including complete context prompt, thought content, and revision instructions.

C Broader Impact

This paper introduces ChronoSteer, a multimodal TSFM that can be steered through textual instructions, effectively bridging LLM and TSFM. After integrating with an LLM, ChronoSteer concurrently leverages both temporal and textual information for future inference, showcasing broad applications in finance, transportation, energy, healthcare, and climate science. Additionally, we propose a two-stage training strategy based on synthetic data to address the scarcity of cross-modal paired data, along with a high-quality MTSF benchmark to prevent information leakage during evaluation.

This work focuses solely on algorithm design and dataset creation. Use of all codes and datasets adheres strictly to their respective licenses (Appendix A.1 and Appendix A.2). There is no ethical risk or negative social impact associated with this research. To facilitate open science and community collaboration, we will make all data, source code, and pre-trained weight checkpoints publicly accessible following the release. These resources will offer substantial support for subsequent research. We believe ChronoSteer will serve as a foundation tool for MTSF, inspiring further advancements in methods and datasets within this field.

D Limitation

Although ChronoSteer demonstrates promising performance by concurrently leveraging both temporal and textual information for future inference, several limitations persist.

First, the paper pays relatively limited attention to transforming textual events into revision instructions. With continuous advancements in LLMs, semantic transformation accuracy is expected to improve steadily, offering strong support for our system. Moreover, after fine-tuning, ChronoSteer shows some ability to correct instructions by leveraging historical data (refer to Section 4.3). Based on these observations, this work primarily focuses on building a bridge between LLMs and TSFMs, steering TSFM predictions through textual revision instructions. However, incorporating techniques such as instruction fine-tuning, retrieval-augmented generation, or in-context learning during instruction generation will enhance instruction quality, further improving overall prediction performance of our system.

Second, limited by the scarcity of high-quality cross-modal paired data, this study employs a two-stage training strategy based on synthetic data and confines textual revision instructions to nine anchors. Although this method achieves promising experiment outcomes, its generalization is still restricted. Access to richer real-world datasets could enhance the potential of ChronoSteer and overcome existing performance bottlenecks.

In the future, we will focus on optimizing textual revision instruction generation and building large-scale cross-modal datasets from real-world scenarios to enhance the robustness and practical applicability of system.